ISSN 0018-1439, High Energy Chemistry, 2024, Vol. 58, Suppl. 4, pp. S563–S568. © Pleiades Publishing, Ltd., 2024.

La–Mg–Ni Intermetallics for Hydrogen Storage and Electrochemical Power Sources

A. A. Volodin[a, *], A. N. Lapshin[a], S. V. Shmalii[a], B. P. Tarasov[a], and M. V. Lototskyy[a, b]

[a] *Federal Research Center of Problems of Chemical Physics and Medicinal Chemistry Russian Academy of Sciences, Chernogolovka, Moscow oblast, 142432 Russia*

[b] *University of the Western Cape, HySA Systems Centre of Competence, Belville, 7535 South Africa*

**e-mail: alexvol@icp.ac.ru*

Received September 12, 2024; revised September 12, 2024; accepted September 20, 2024

Abstract—The paper summarizes the results of the studies of La–Mg–Ni based intermetallic compounds for reversible hydrogen sorption and electrochemical applications. The phase composition, hydrogen sorption and electrochemical characteristics of AB_5-, AB_3- and AB_2-types intermetallic compounds are considered. A comparative evaluation of the materials is carried out. It has been shown that the maximum capacity of electrodes with AB_3-type intermetallic compounds reaches 400 mA h/g, which is 25% higher than the capacity of electrodes based on AB_5-type (315 mA h/g) and 7.5% higher than the capacity of electrodes with AB_2-type intermetallic compound (370 mA h/g). AB_2-type intermetallic compounds demonstrate good performance at high discharge current densities, and the presence of lanthanum promotes rapid activation of the electrodes.

Keywords: hydrogen, hydride, intermetallic, hydrogen sorption, anode materials, electrochemical capacity, Ni-MH battery

DOI: 10.1134/S0018143924701637

INTRODUCTION

Various intermetallic compounds (IMCs) of the AB_5, $AB_{3-3.5}$, and AB_2-types (where A is a rare earth metal and B is a transition metal) are actively used as working materials for hydrogen storage systems and Ni-MH power sources [1–5]. The hydrogen sorption capacity of $LaNi_5H_{6.6}$ hydride is ~1.4 wt %, and electrochemical power sources based on Co-doped $LaNi_5$ surpass Ni-Cd batteries in capacity, service life, resistance to overcharge, and environmental friendliness [6]. AB_5-type compounds have high catalytic activity and cyclic stability, but their electrochemical capacity is limited (~300 mA h/g). AB_2-type IMCs have higher capacity characteristics (~350 mA h/g), but this type of compounds requires long-term activation. IMCs $AB_{3-3.5}$ demonstrate higher electrochemical capacity (350–400 mA h/g) compared to traditional AB_5-type IMCs, but their cyclic stability is greatly reduced during oxidation and corrosion in an alkaline electrolyte (15–20% of the initial value for every 100 cycles). In order to increase hydrogen sorption and electrochemical capacities, as well as cyclic stability, intermetallic compounds are usually alloyed with lighter elements, such as Mg [7]. Magnesium and its alloys have high hydrogen capacity (~ 7.5 wt % H), but the high temperatures required for hydrogen desorption and the corrosion instability of magnesium in an alkaline electrolyte make it difficult to use these alloys. Previous studies have shown that AB_5-type intermetallic compounds containing La, Ce, Nd, Ni, Co, Mn, Cr, and Al have a low equilibrium hydrogen desorption pressure (~0.1 bar at 20°C). The hydrogen capacity is in the range of 1.0–1.3 wt %. Electrodes with intermetallic compounds are easily activated, and the maximum capacity is 300–325 mA h/g [8]. Intermetallic compounds $(La,Nd,Mg)Ni_3$ with the $PuNi_3$ structure have higher hydrogen sorption and electrochemical characteristics compared to AB_5-type IMCs [9–12]. Hydride phases in the $LnNi_3–H_2$ system are formed at a lower hydrogen pressure than in the $LnNi_5–H_2$ systems and have a 23% higher hydrogen capacity. The capacity of electrodes with the $La_{1.5}Nd_{0.5}MgNi_9$ alloy is 400 mA h/g at a discharge current density of 100 mA/g, which is also 23% higher than that of $LnNi_5$. After 300 charge-discharge cycles at 300 mA/g, the capacity of electrodes with $(La,Nd,Mg)Ni_3$ compounds was 76% of the initial capacity, which confirms good cyclic stability. Intermetallics of the AB_2 type with the Laves phase structure demonstrate high performance characteristics and cyclic stability, which makes them promising materials for electrodes of metal hydride power sources. The problem of long-term activation of electrodes can be solved by introducing various additives

into the intermetallics, such as La and Ni. We have obtained a series of IMCs (Ti-Zr)(Ni–Mn–V–Fe)$_{2\pm x}$ with a catalytic additive (~1 wt %) La [13, 14]. Such IMCs have a low (~1 bar at 20°C) plateau pressure of hydrogen absorption and desorption and a small hysteresis value. The hydrogen capacity is 1.54 wt %. Electrodes based on the studied alloys are quickly activated and reach a maximum capacity (370 mA h/g at 100 mA/g) by the fourth charge-discharge cycle. With a 10-fold increase in the discharge current density (1000 mA/g), the electrode capacity is 246 mA h/g (65% of the initial). After 100 charge-discharge cycles at 300 mA/g, the IMCs retain more than 90% of the initial capacity. It has also been shown that Ni clusters deposited on the surface of carbon nanomaterials catalyze the processes of hydrogen sorption-desorption and electrode charge-discharge [15, 16].

The aim of present work is a comparative analysis of the hydrogen sorption and electrochemical characteristics of AB_3-type (La,Nd,Mg)Ni_9, AB_2-type (Ti,Zr,La)(Ni,Mn,V,Fe)$_2$ intermetallic compounds and their comparison with the data obtained for the $LaNi_5$ and $LaNi_{4.45}Al_{0.55}$ IMCs (AB_5-type).

Phase Composition of Intermetallics

The main problem in smelting intermetallics is to obtain homogeneous single-phase samples. As a rule, AB_5-type intermetallics are smelted with a high degree of homogeneity and contain only one phase with the $CaCu_5$ structure [8]. Such IMCs rarely require further processing. A similar situation is observed in the case of AB_2-type IMCs. The cast alloys contain the C15 phase with the FCC structure of the $MgCu_2$-type as the main phase and C14 with the hexagonal structure as the secondary phase [13]. A more complex picture is observed in the production of AB_3-type intermetallics. The cast alloys, along with the main phase of the $PuNi_3$ structural type, contain the secondary A_2B_7 (Gd_2Co_7-type) and A_5B_{19} (Ce_5Co_{19}-type) phases [9]. One of the ways to solve this problem may be long-term annealing of cast alloys in an argon atmosphere at 950°C followed by quenching in cold or ice water [9–13]. This procedure reduces the amount of secondary phases up to their complete disappearance. Partial replacement of La by Mg in intermetallic compounds $(La,Mg)_3Ni_9$ leads to a decrease in the unit cell volume, which is associated with a smaller atomic radius of magnesium (1.60 Å) compared with the radius of lanthanum (1.87 Å). On the contrary, partial replacement of Ni atoms by Al in AB_5-type intermetallic compounds increases the volume of the unit cell, since the atomic radius of aluminum (1.43 Å) is larger than that of nickel (1.24 Å). It should be noted that all phases present in the alloys are capable of reversibly absorbing hydrogen. The impurity phase A_2B_7, which most often accompanies the AB_3 phase, has hydrogen sorption characteristics similar to it.

Hydrogen Sorption Characteristics of Intermetallics

All AB_3-type intermetallics are characterized by lower hydride formation pressure than $Ti_{0.15}Zr_{0.85}La_{0.03}Ni_{1.2}Mn_{0.7}V_{0.12}Fe_{0.12}$ and $LaNi_5$ (Fig. 1). However, the plateau of hydrogen equilibrium pressure in AB_5 and AB_2-type alloys has a much smaller slope, which indicates a greater degree of homogeneity of these alloys and the absence or insignificant presence of secondary phases, in contrast to AB_3-type alloys. In addition, AB_2-type alloys have a smaller hysteresis compared to other alloys, which indicates the flexibility of the alloy crystal lattice in the process of hydrogen sorption-desorption.

An increase in the magnesium content in AB_3-type intermetallic compounds leads to an increase in the equilibrium hydrogen pressure, which is associated with a decrease in the volume of the crystal lattice, while the plateau slope angle decreases. Partial replacement of Ni atoms by Al in AB_5-type IMCs leads to a decrease in the equilibrium pressure by an order of magnitude, which can be useful for hydrogen sorption with low partial pressure. Analysis of the obtained isotherms showed that the maximum reversible hydrogen capacity for AB_3-type alloys is 10% higher than for $LaNi_5$ (1.4 wt % H) and by 2% compared to $Ti_{0.15}Zr_{0.85}La_{0.03}Ni_{1.2}Mn_{0.7}V_{0.12}Fe_{0.12}$ (1.54 wt % H). The maximum capacity value was recorded for the $La_{1.5}Nd_{0.5}MgNi_9$ alloy (1.57 wt % H), which corresponds to 13 hydrogen atoms per formula unit of the hydride. In addition, in the $La_{1.5}Nd_{0.5}MgNi_9$–H_2 system, the plateau of the phase transition of the α-solution to the β-hydride is flatter than in the La_2MgNi_9–H_2 system. This behavior may be due to the greater homogeneity of the alloy and the lower content of impurity phases in the alloy.

Hydrogen Diffusion in Hydrides

For all the studied alloys, the maximum value of the hydrogen diffusion coefficient was observed at 15–20% of the charge state (Fig. 2, shown using the data for La_2MgNi_9 and $La_{1.5}Nd_{0.5}MgNi_9$ as an example). Subsequently, as saturation occurs, the hydrogen diffusion rate in the alloys decreases by almost two orders of magnitude, which is associated with the filling of free voids and, as a consequence, the difficulty of atomic hydrogen penetration into the metal particle. As can be seen from Fig. 2, the maximum D_H value for $La_{1.5}Nd_{0.5}MgNi_9$ is achieved already at a saturation state of 15% and is 2.9×10^{-11} cm^2/s, while for La_2MgNi_9 this value is 1.3×10^{-11} cm^2/s. The difference in D_H increases as the charge state increases. This behavior can probably be associated with the presence of impurity phase regions in the La_2MgNi_9 alloy, which can somewhat slow down the effective hydrogen diffusion. The maximum value of the hydrogen diffusion coefficient for $La_{1.9}Mg_{1.1}Ni_9$, as in the case of

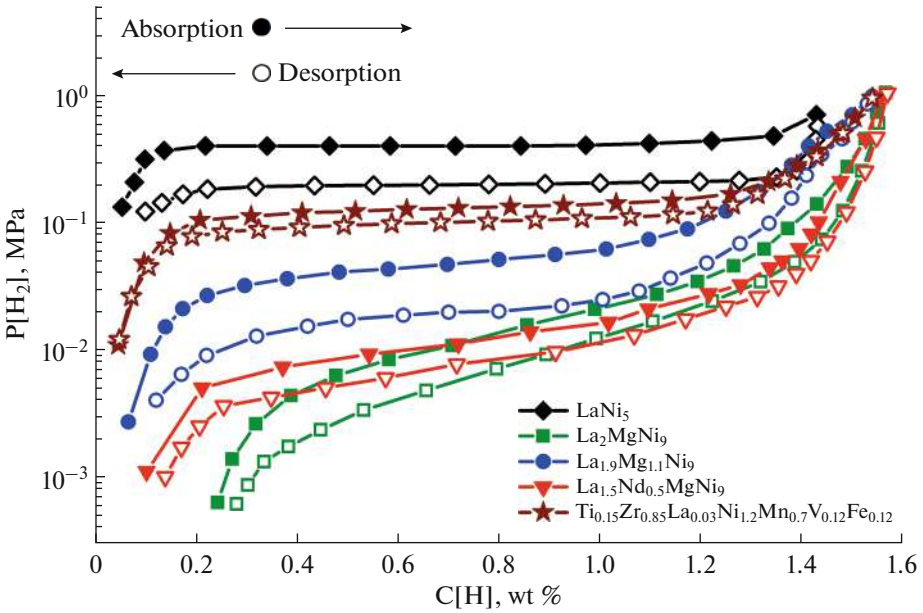

Fig. 1. P–C isotherms of hydrogen absorption-desorption for IMCs AB_5, AB_3 and AB_2 types measured at 25°C.

La_2MgNi_9, is 1.1 × 10^{-11} cm^2/s, for $LaNi_5$ $D_H = 8.7 \times 10^{-12}$ cm^2/s, and the lowest D_H value (4.3×10^{-13} cm^2/s) was obtained for $Ti_{0.15}Zr_{0.85}La_{0.03}Ni_{1.2}Mn_{0.7}V_{0.12}Fe_{0.12}$.

Electrochemical Characteristics of Intermetallids

Metal hydride electrodes with AB_3-type alloys demonstrate high specific capacity and performance at high current densities (Fig. 3). The capacity of the electrode with $La_{1.5}Nd_{0.5}MgNi_9$ alloy was 400 mA h/g at a discharge current density of 50 mA/g, which is 35% higher than that of the $LaNi_5$ alloy used in commercial electrodes (295 mA h/g) and 7.5% higher than that of AB_2 alloy (370 mA h/g). For electrodes with La_2MgNi_9 and $La_{1.9}Mg_{1.1}Ni_9$ alloys, the maximum capacity was 390 and 380 mA h/g, respectively. The calculated content of hydrogen released from the alloy hydrides was: 1.17 wt % for $LaNi_5H_x$, 1.44 wt % for $La_2MgNi_9H_x$, and 1.42 and 1.47 wt % for $La_{1.9}Mg_{1.1}Ni_9H_x$ and $La_{1.5}Nd_{0.5}MgNi_9H_x$, respectively. Some difference between the electrochemical data and the values obtained in the gas phase can be explained by the fact that the electrochemical process of hydrogen sorption-desorption occurs, unlike the gas-phase process, at atmospheric pressure and some hydrogen does not participate in the process. In addition, it is necessary to take into account the electrochemical processes occurring at the electrode-electrolyte phase boundary, which make a significant contribution during the charge-discharge of the electrodes. In general, the data obtained for electrochemical and gas-phase measurements are in good agreement with each other. It is worth noting that the plateau on the discharge curve in the section from–0.9 to–0.85 V for the Nd-containing alloy is flatter and longer than for other alloys. These data are in good agreement with the equilibrium pressure curves obtained in the gas phase. In addition, electrodes with Nd-containing intermetallic have higher values of specific capacity with an increase in the discharge current density from 50 to 850 mA/g (Fig. 4).

With an increase in the current density from 50 to 1000 mA/g, the capacity of the electrodes decreases by 60% of the initial value. The maximum value of specific capacity was obtained for the AB_2 alloy

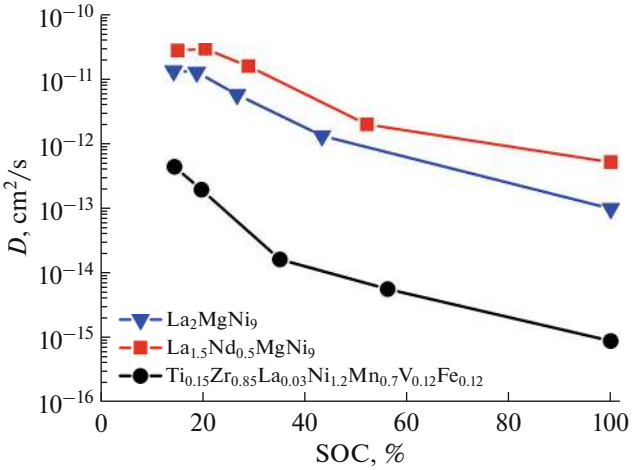

Fig. 2. Dependence of hydrogen diffusion coefficient on the state of charge for alloys AB_3 and AB_2-types.

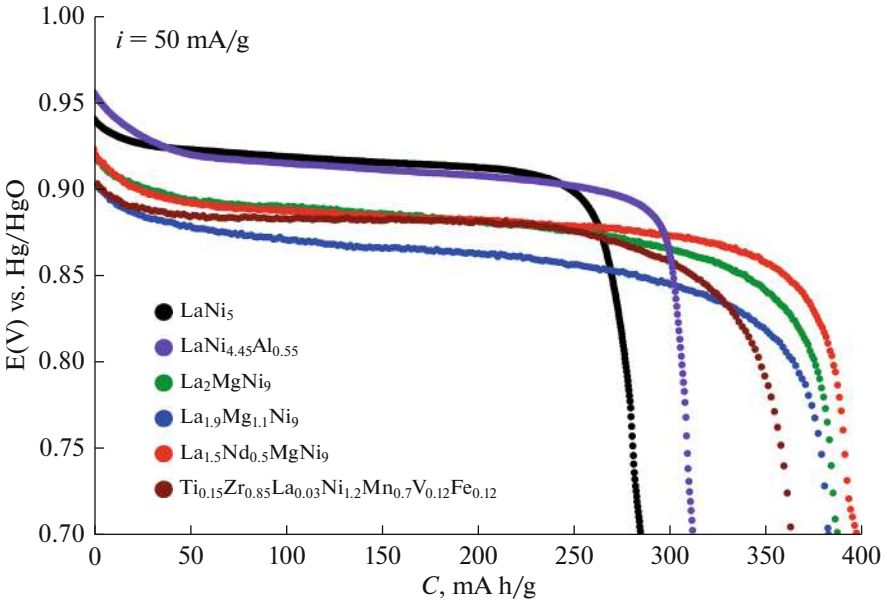

Fig. 3. Specific capacity of electrodes at 25°C and at discharge current density of 50 mA/g.

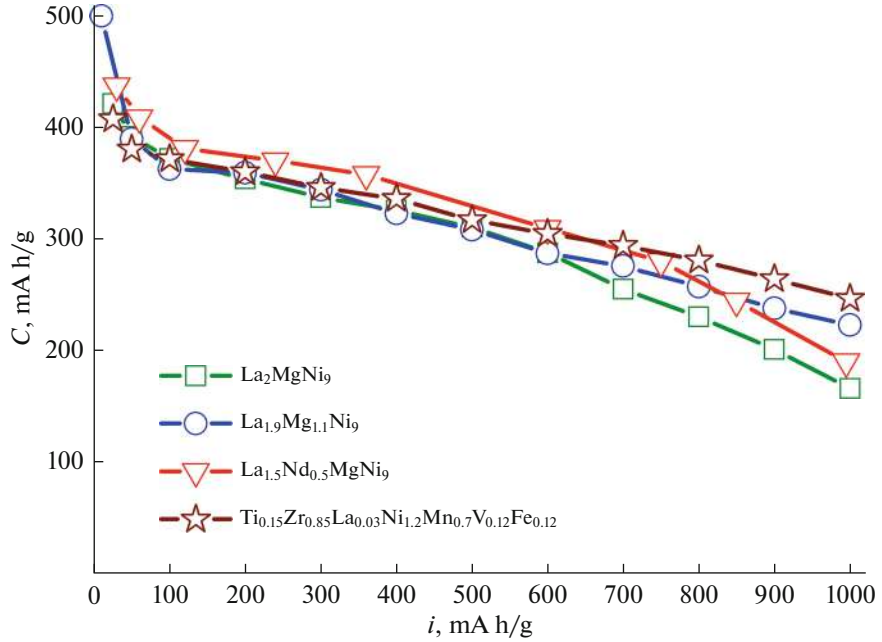

Fig. 4. Dependence of the specific capacity for electrodes on the discharge current density.

(246 mA h/g at a current density of 1000 mA/g). The capacity of MH electrodes at a high discharge current density can be increased by improving the electrical conductivity of the anode, for example, by adding graphene. Thus, in work [17], it was possible to maintain up to 90% of the capacity with a fivefold increase in current density using a composite material based on the $La_{11.3}Mg_{6.0}Sm_{7.4}Ni_{61.0}Co_{7.2}Al_{7.1}$ alloy with graphene. In work [18] it was shown that the addition of carbon nanofibers to lanthanum oxide increases the electrical conductivity of the composite by more than two orders of magnitude.

With increasing current density from 50 to 1000 mA/g the electrodes capacity is reduced by 60% from the initial value. Capacity of MH-electrodes at high discharge current density can be increased by improving the electrical conductivity of the anode for example by adding graphene. In [29] authors managed

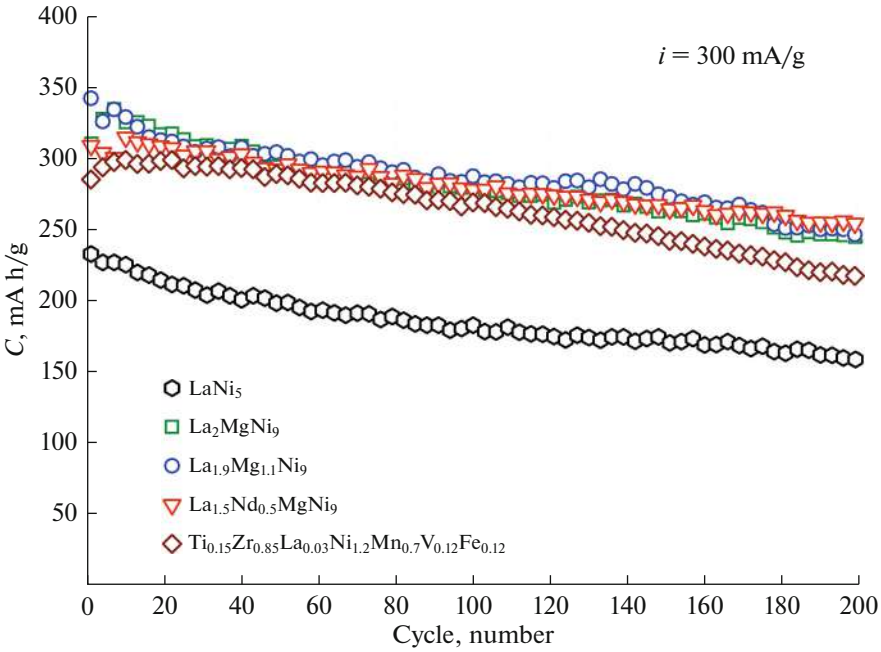

Fig. 5. Cyclic stability of electrodes at a discharge current density of 300 mA/g.

to retain up to 90% of capacity with increasing current density in five times by using a composite material based on $La_{11.3}Mg_{6.0}Sm_{7.4}Ni_{61.0}Co_{7.2}Al_{7.1}$ alloy with graphene. In [30] it was shown that the addition of carbon nanofibers to lanthanum oxide increases the electrical conductivity of the composite more than two orders.

All electrodes with AB_3-type intermetallic compounds show satisfactory cyclic stability (Fig. 5). The study of the electrode stability at a discharge current density of 300 mA/g (1C) over 200 cycles shows that the drop in specific capacity is about 30%, which is slightly higher than for $LaNi_5$, but the capacity after 200 cycles still remains significantly higher than for the specified comparison sample.

The cyclic degradation of the electrodes is apparently associated with the oxidation of Mg and La in $La_{3-x}Mg_xNi_9$, which leads to the formation of $Mg(OH)_2$ and $La(OH)_3$ hydroxides on the surface of intermetallic particles during charging and discharging [19, 20]. The corrosion behavior of the active components depends on the temperature, electrolyte concentration, discharge current density and discharge potential. The influence of these factors on the corrosion rate of the alloy surface and cyclic stability requires further research.

CONCLUSIONS

Partial substitution of Ni atoms by Al in AB_5-type intermetallics increases the unit cell volume and decreases the equilibrium hydrogen pressure by an order of magnitude. An increase in the Mg content in $La_{3-x}Mg_xNi_9$ intermetallics leads to a decrease in the unit cell volume. Partial replacement of La by Nd promotes the formation of an alloy with a predominant content of the AB_3 phase. For the $La_{1.5}Nd_{0.5}MgNi_9$–H_2 system, the phase transition of the α-solid solution to the β-hydride is characterized by a flatter and wider plateau both in the process of hydrogen absorption and desorption and during electrochemical charging and discharging. The maximum capacity of the electrodes with Nd-containing alloy is 400 mA h/g at a discharge current density of 60 mA/g, which is 35% higher than the capacity of the electrodes based on $LaNi_5$ (295 mA h/g) and 7.5% higher than the capacity of the electrodes with AB_2-type alloy (370 mA h/g). The La-containing AB_2-type intermetallic compound demonstrates good performance at high discharge current densities, but its capacity and cyclic stability are slightly lower compared to AB_3-type alloys.

FUNDING

The work was carried out under the support from the Ministry of Science and Higher Education of the Russian Federation (Megagrant, Agreement number 075-15-2022-1126, signed on July 1, 2022).

CONFLICT OF INTEREST

The authors of this work declare that they have no conflicts of interest.

REFERENCES

1. Wan, C.B., Denys, R.V., and Yartys, V.A., *J. Alloys Compd.*, 2021, vol. 889, p. 161655.
2. He, X., Xiong, W., Wang, L., et al., *J. Alloys Compd.*, 2022, vol. 921, p. 166064.
3. Liu, Y., Yuan, H., and Jiang, L., *Int. J. Hydrogen Energy*, 2019, vol. 44, p. 22064.
4. Wan, C.B., Denys, R.V., and Yartys, V.A., *Dalton Trans.*, 2022, vol. 51, p. 12986.
5. Zhang, Y., Wei, X., Gao, J., et al., *Electrochim. Acta*, 2020, vol. 342, p. 136123.
6. Yartys, V., Noreus, D., and Latroche, M., *Appl. Phys. A*, 2016, vol. 122, p. 1.
7. Liu, T., Chen, Ch., Qin, Ch., and Li, X., *Int. J. Hydrogen Energy*, 2014, vol. 39, p. 18273.
8. Kazakov, A.N., Blinov, D.V., Bodikov, V.Y., et al., *Int. J. Hydrogen Energy*, 2021, vol. 46, p. 13622.
9. Volodin, A.A., Wan, Ch., Denys, R.V., et al., *Int. J. Hydrogen Energy*, 2016, vol. 41, p. 9954.
10. Volodin, A.A., Fursikov, P.V., Fokina, E.E., and Tarasov, B.P., *Russ. J. Phys. Chem. A*, 2020, vol. 94, p. 1017.
11. Tarasov, B.P., Fursikov, P.V., Volodin, A.A., et al., *Int. J. Hydrogen Energy*, 2021, vol. 46, p. 13647.
12. Volodin, A.A., Lapshin, A.N., Yakushin, I.O., and Tarasov, B.P., *High Energy Chem.*, 2023, vol. 57, Suppl. 2, p. S370.
13. Volodin, A.A., Denys, R.V., Wan, C.B., et al, *J. Alloys Compd.*, 2019, vol. 793, p. 564.
14. Wijayanti, I.D., Denys, R., Suwarno, S., et al, *J. Alloys Compd.,* 2020, vol. 828, p. 154354.
15. Tarasov, B.P., Arbuzov, A.A., Volodin, A.A., et al., *J. Alloys Compd.*, 2022, vol. 896, p. 162881.
16. Tarasov, B., Arbuzov, A., Mozhzhukhin, S., et al., *Inorganics*, 2023, vol. 11, p. 290.
17. Ouyang, L.Z., Cao, Z.J., Li, L.L., et al., *Int. J. Hydrogen Energy*, 2014, vol. 39, p. 12765.
18. Li, P., Zhao, Y., Yu, B., et al., *Int. J. Hydrogen Energy*, 2015, vol. 40, p. 9783.
19. Hu, W.K., Denys, R.V., Nwakwuo, C.C., et al., *Electrochim. Acta*, 2013, vol. 96, p. 27.
20. Ma, Z., Zhu, D., Wu, C., et al., *J. Alloys Compd.*, 2015, p. 149.